Inorganic Chemistry

Article

pubs.acs.org/IC

Metal–Organic Frameworks Based on Previously Unknown Zr_8/Hf_8 Cubic Clusters

Dawei Feng,[†,§] Hai-Long Jiang,[†,‡,§] Ying-Pin Chen,[†] Zhi-Yuan Gu,[†] Zhangwen Wei,[†] and Hong-Cai Zhou*[,†]

[†]Department of Chemistry, Texas A&M University, College Station, Texas 77843, United States

[‡]Hefei National Laboratory for Physical Sciences at the Microscale, Department of Chemistry, University of Science and Technology of China, Hefei, Anhui 230026, P.R. China

Supporting Information

ABSTRACT: The ongoing study of zirconium– and hafnium–porphyrinic metal–organic frameworks (MOFs) led to the discovery of isostructural MOFs based on Zr_8 and Hf_8 clusters, which are unknown in both cluster and MOF chemistry. The Zr_8O_6 cluster features an idealized Zr_8 cube, in which each Zr atom resides on one vertex and each face of the cube is capped by one μ_4-oxygen atom. On each edge of the cube, a carboxylate from a porphyrinic ligand bridges two Zr atoms to afford a 3D MOF with a very rare (4,12)-connected **ftw** topology, in which two types of polyhedral cages with diameters of ~1.1 and ~2.0 nm and a cage opening of ~0.8 nm are found. The isostructural Zr– and Hf–MOFs exhibit high surface areas, gas uptakes, and catalytic selectivity for cyclohexane oxidation.

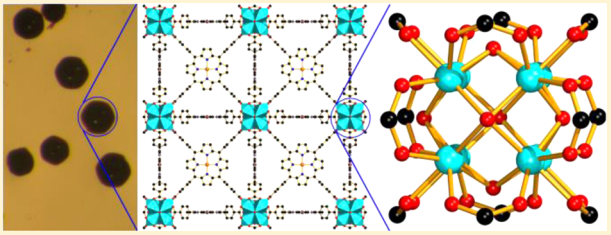

INTRODUCTION

Metal–organic frameworks (MOFs) are extended structures assembled from metal-containing units (metal cations or clusters) and organic linkers.[1] As a new class of porous materials, MOFs have attracted tremendous attention in the past two decades. One of the main reasons is their application potential in gas storage/separation, catalysis, sensing, and drug delivery,[2−5] thanks to their exceptionally high surface area as well as adjustable pore shape, size, and functionality. In the construction of MOFs, going from simple metal ions to more complicated metal-containing units (M_2 paddlewheel, M_3O and M_4O basic carboxylates) represents a significant initial step.[1a,b,6] The utilization of a new metal cluster as a structural unit often led to a series of new MOFs. In general, the introduction of metal clusters of high nuclearity has led to MOFs with improved stability, which is a prerequisite for industrial applications. Although only a limited number of Zr-based MOFs were reported,[7] they have unambiguously shown improved stability compared to the common Zn/Cu/Cd-based carboxylate MOF. Robust MOFs based on Zr clusters with high porosity are very desirable for practical applications. However, it is particularly difficult to obtain single crystals of Zr-based MOFs due to the inert coordination bonds between Zr^{4+} cations and carboxylate anions, making ligand-exchange reactions extremely slow, which is unfavorable for defect repair during crystal growth. To meet such a challenge, a modulated synthetic strategy was adopted and benzoic acid was introduced to the reaction mixture.[7b,e,f] Such a synthetic strategy has greatly facilitated crystal growth for the study of Zr–MOFs; however, only a few MOFs containing Zr clusters have been reported, and almost all of them are based on the octahedral Zr_6 cluster.

So far in cluster chemistry, Zr_3, Zr_4, Zr_5, Zr_6, and Zr_{10} clusters have been synthesized and characterized.[6a,8] Due to very similar radii of Hf^{4+} and Zr^{4+} cations, polyoxohafnium clusters of Hf_3, Hf_4, Hf_6, Hf_{17}, and Hf_{18} have also been reported.[6a,8b,9] Most of these clusters are difficult to be incorporated into MOF structures due to symmetry limitations. To the best of our knowledge, only Zr_6 clusters[7a−g] and zirconium oxide chains[7h] have been introduced into Zr–MOFs. Only one Hf–MOF[7e] containing Hf_6 clusters was reported. In our continuing search for ultrastable Zr– and Hf–MOFs, with tetrakis(4-carboxyphenyl)porphyrin (TCPP) as an organic linker, a series of MOFs supported by previously unknown Zr_8 and Hf_8 cubic clusters have been isolated and structurally characterized. The MOFs exhibit high surface area and interesting gas-sorption properties. In particular, a Zr_8–MOF constructed from an Fe–TCPP ligand was tested as a catalyst for cyclohexane oxidation, which revealed very high selectivity toward cyclohexanone and cyclohexanol formation using neat cyclohexane.

EXPERIMENTAL SECTION

Materials and Instrumentation. Methyl 4-formylbenzoate was purchased from Oakwood Products, Inc. Pyrrole, propionic acid, *N*,*N*-dimethylformamide (DMF), *N*,*N*-diethylformamide (DEF), benzoic acid, acetone, zirconium(IV) chloride, hafnium(IV) chloride, iron(II) chloride tetrahydrate ($FeCl_2·4H_2O$), copper(II) chloride tetrahydrate ($CuCl_2·4H_2O$), cobalt(II) chloride hexahydrate ($CoCl_2·6H_2O$),

Received: July 17, 2013
Published: October 22, 2013

   dx.doi.org/10.1021/ic4018536 | *Inorg. Chem.* 2013, 52, 12661−12667

Scheme 1. Synthetic Route for M−TCPP Ligands

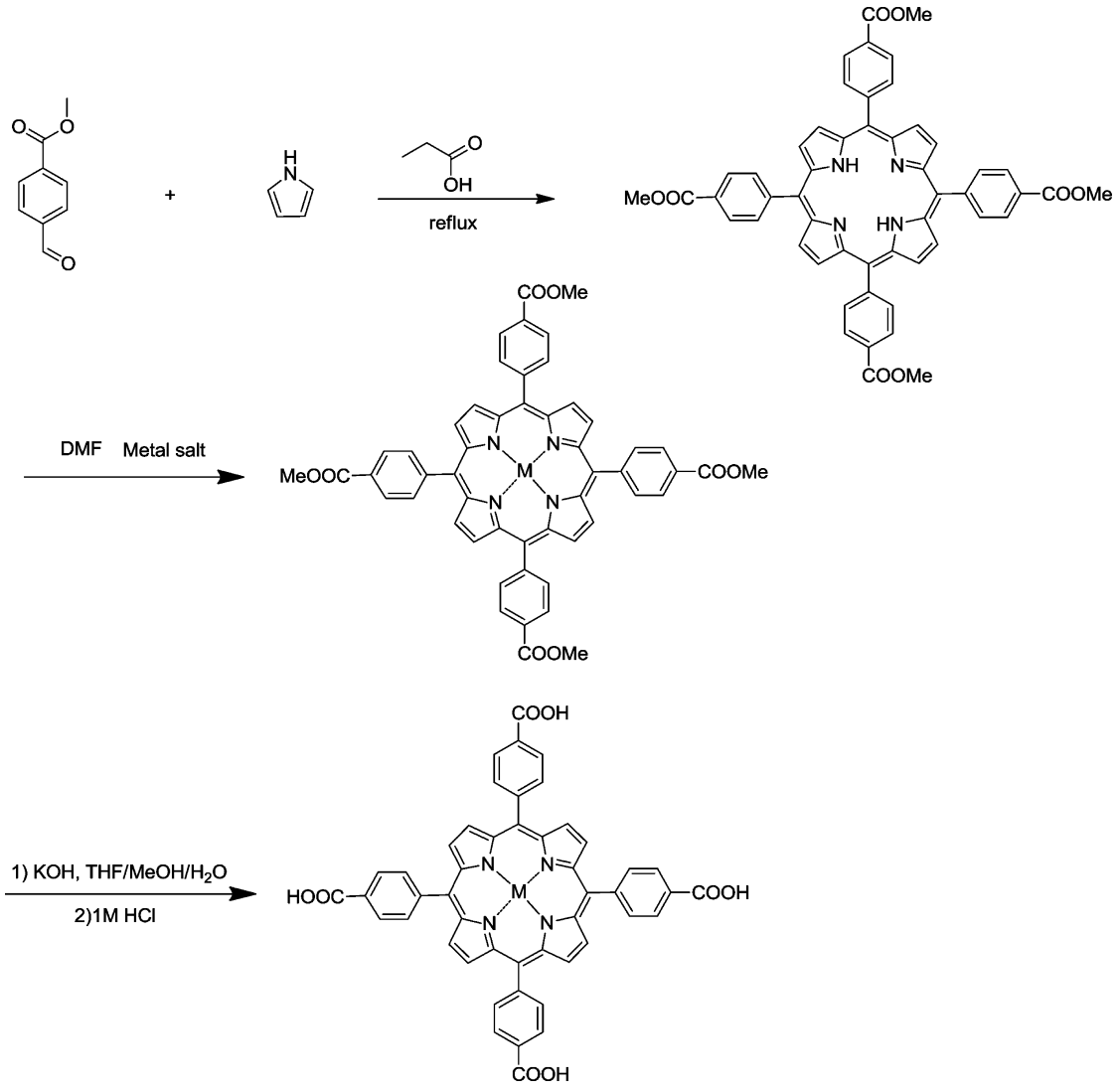

chlorobenzene, *tert*-butyl hydroperoxide, and cyclohexane were purchased from Alfa Aesar. 5,10,15,20-Tetrakis(4-methoxycarbonylphenyl)porphyrin (TPPCOOMe) was prepared according to the procedures described below. All commercial chemicals were used without further purification unless otherwise mentioned.

Powder X-ray diffraction (PXRD) was carried out with a BRUKER D8-Focus Bragg−Brentano X-ray powder diffractometer equipped with a Cu-sealed tube (λ = 1.54178) at 40 kV and 40 mA. Elemental analysis (C, H, and N) were performed by Atlantic Microlab, Inc. (Norcross, GA). Thermogravimetry analyses (TGA) were conducted on a TGA-50 (SHIMADZU) thermogravimetric analyzer. Fourier transform infrared (IR) measurements were performed on a SHIMADZU IR Affinity-1 spectrometer. Nuclear magnetic resonance (NMR) data were collected on a Mercury 300 spectrometer. X-ray photoelectron spectra (XPS) were acquired with Axis Ultra DlD (Kratos) equipped with Al monochromatic X-rays operating at 12 kV and 10 mA. Gas sorption measurements were conducted using a Micrometritics ASAP 2420 system at various temperatures. Electron paramagnetic resonance (EPR) spectra for TCPP ligand and Zr-PCN-221(no metal) were recorded on a Varian E-line 12″ Century Series X-band CW spectrometer.

Ligand Synthesis. The tetrakis(4-carboxyphenyl)porphyrin (H_2TCPP) and [5,10,15,20-tetrakis(4-carboxyphenyl)porphyrinato]-Cu(II) (CuTCPP) ligands were directly purchased from Frontier Scientific. Other metal-involved TCPP (M−TCPP) ligands were all synthesized based on previous reports with slight modifications. The syntheses of these ligands have been previously described.[7g] Typically, we obtained these ligands by three steps as shown in Scheme 1.

5,10,15,20-Tetrakis(4-methoxycarbonylphenyl)porphyrin (TPPCOOMe). In a 500-mL three necked flask, methyl *p*-formylbenzoate (6.9 g, 0.042 mol) was dissolved in propionic acid (100 mL). Pyrrole was then added dropwise (3.0, 0.043 mol), and the solution was refluxed for 12 h in darkness. After the reaction mixture was cooled to room temperature, purple crystals were collected by suction−filtration. (1.9 g, 2.24 mmol, 21% yield). ^{1}H NMR (300 MHz, $CDCl_3$): δ 8.81 (s, 8H), 8.43 (d, 8H), 8.28 (d, 8H), 4.11 (s, 12H), −2.83 (s, 2H).

5,10,15,20-Tetrakis(4-methoxycarbonylphenyl)porphyrin−M (M−TPPCOOMe). [5,10,15,20-Tetrakis(4-methoxycarbonylphenyl)-porphyrinato]Fe(III) Chloride. TPP-COOMe (0.854 g, 1.0 mmol) and $FeCl_2{\cdot}4H_2O$ (2.5 g, 12.8 mmol) were added into 100 mL of DMF, and the mixture was refluxed for 6 h. After being cooled to room temperature, 150 mL of H_2O was introduced. The resultant precipitate was filtered and washed with 50 mL of H_2O twice. The obtained solid was dissolved in $CHCl_3$, washed three times with 1 M HCl, and twice with water. The organic layer was then dried over anhydrous magnesium sulfate and evaporated to give dark brown crystals in almost quantitative yield.

[5,10,15,20-Tetrakis(4-methoxycarbonylphenyl)porphyrinato]Co-(II). TPP-COOMe (0.854 g, 1.0 mmol) and $CoCl_2{\cdot}6H_2O$ (3.1 g, 12.8 mmol) were added into 100 mL of DMF, and the mixture was refluxed

dx.doi.org/10.1021/ic4018536 | *Inorg. Chem.* 2013, 52, 12661−12667

for 6 h. After the mixture was cooled to room temperature, 150 mL of H_2O was introduced. The resultant precipitate was filtered and washed with 50 mL of H_2O twice. The obtained dark red solid was dissolved in $CHCl_3$ and washed three times with distilled water. The organic layer was then dried over anhydrous magnesium sulfate and evaporated to give red crystals in almost quantitative yield.

[5,10,15,20-Tetrakis(4-carboxyphenyl)porphyrinato]M (M–TCPP). [5,10,15,20-Tetrakis(4-carboxyphenyl)porphyrinato]Fe(III) Chloride. The obtained ester (0.75 g) was stirred in a mixed solvent of THF (25 mL) and MeOH (25 mL), to which a solution of KOH (2.63 g, 46.95 mmol) in H_2O (25 mL) was added. The mixture was then refluxed for 12 h. After the mixture was cooled to room temperature, THF and MeOH were evaporated. Additional water was added to the resultant water phase. and the mixture was slightly heated until the solid was fully dissolved, and then the homogeneous solution was acidified with 1 M HCl until no further precipitate was produced. The brown solid was collected by filtration, washed with water three times, and dried in a vacuum oven. FTIR (KBr, cm^{-1}): 3444 (m), 3034 (w), 2634 (w), 1702 (s), 1614 (s), 1570 (m), 1404 (s), 1311 (m), 1277 (s), 1204 (m), 1180 (m), 1106 (m), 1004 (s), 862 (m), 799 (s), 770 (s), 721 (m).

[5,10,15,20-Tetrakis(4-carboxyphenyl)porphyrinato]Co(II). The obtained ester (0.75 g) was stirred in a mixed solvent of THF (25 mL) and MeOH (25 mL), to which a solution of KOH (2.63 g, 46.95 mmol) in H_2O (25 mL) was added. This mixture was refluxed for 12 h. After the mixture was cooled to room temperature, THF and MeOH were evaporated. Additional water was added to the resultant water phase and the mixture was slightly heated until the solid was fully dissolved, then the homogeneous solution was acidified with 1 M HCl until no further precipitate was produced. The red solid was collected by filtration, washed with water, and dried under a vacuum. FTIR (KBr, cm^{-1}): 3423 (m), 2950 (w), 2840 (w), 1719 (s), 1605 (s), 1546 (m), 1458 (m), 1394 (s), 1351 (m), 1276 (s), 1177 (w), 1112 (s), 1002 (s), 868 (w), 833 (m), 798 (s), 716 (m).

Synthesis of Zr–PCN-221(no metal). $ZrCl_4$ (7 mg), H_2TCPP (10 mg), and 7 drops of acetic acid or trifluoroacetic acid (80 μL) in 2 mL of DEF were ultrasonically dissolved in a Pyrex vial. The mixture was heated in a 120 °C oven for 12 h. After the mixture was cooled to room temperature, a dark red powder was harvested by filtration (10 mg, 71% yield). FTIR (KBr, cm^{-1}): 1735 (w), 1664 (vs), 1587 (m), 1548 (m), 1408 (vs), 1257 (w), 1209 (w), 1185 (w), 1158 (w), 1099 (s), 1022 (w), 968 (s), 837 (w), 811 (m), 775 (s), 722 (m), 662 (vs). Anal. Calcd for Zr–PCN-221(No metal): C, 52.29; H, 2.47; N, 5.28. Found: C, 50.34; H, 2.84; N, 5.81.

Synthesis of Zr–PCN-221(Fe). $ZrCl_4$ (7 mg), Fe–TCPPCl (10 mg), and 7 drops of acetic acid or trifluoroacetic acid (80 μL) in 2 mL of DEF were ultrasonically dissolved in a Pyrex vial. The mixture was heated in 120 °C oven for 12 h. After the mixture was cooled to room temperature, dark brown powder was harvested by filtration (10 mg, 70% yield). FTIR (KBr, cm^{-1}): 1738 (w), 1607 (s), 1545 (m), 1414 (vs), 1346 (w), 1182 (w), 1150 (w), 1102 (w), 998 (s), 870 (w), 805 (s), 776 (s), 710 (m), 671 (s). Anal. Calcd for Z–PCN-221(Fe): C, 51.67; H, 2.17; N, 5.02. Found: C, 50.72; H, 2.12; N, 4.84.

Synthesis of Zr–PCN-221(Cu). $ZrCl_4$ (10 mg), CuTCPP (10 mg), and benzoic acid (250 mg) in 2 mL of DMF were ultrasonically dissolved in a Pyrex vial. The mixture was heated in a 120 °C oven for 12 h. After being cooled to room temperature, the mixture of dark red needles and cubic crystals were harvested. The red needle phase has been demonstrated to be PCN-222[7g] by powder X-ray diffraction. The cubic crystal, which is PCN-221, has been characterized by single-crystal X-ray diffraction.

Synthesis of Hf–PCN-221(Co). $HfCl_4$ (30 mg), CoTCPP (10 mg) and benzoic acid (400 mg) in 2 mL of DMF were ultrasonically dissolved in a Pyrex vial. The mixture was heated in a 120 °C oven for 8 h. After the mixture was cooled to room temperature, red cubic crystals were harvested by filtration (10 mg, 47% yield). FTIR (KBr, cm^{-1}): 1750 (w), 1685 (m), 1643 (w), 1610 (w), 1548 (s), 1512 (s), 1414 (s), 1379 (m), 1340 (w), 1269 (w), 1150 (w), 1040 (m), 870 (w), 838 (w), 775 (w), 722 (m). Anal. Calcd for Hf–PCN-221(Co): C, 42.65; H, 1.79; N, 4.15. Found: C, 41.81; H, 2.40; N, 3.30.

X-ray Crystallography. A crystal was taken directly from the mother liquor, transferred to oil, and mounted into a loop for single-crystal X-ray data collection, which was conducted on a Bruker Smart Apex diffractometer equipped with a low temperature device (under 110 K) and an Mo Kα sealed-tube X-ray source (λ = 0.71073 Å, graphite monochromator). The data frames were collected using the program APEX2 and processed using the program SAINT routine within APEX2. The data were corrected for absorption and beam correction based on the multiscan technique as implemented in SADABS. The structures were solved by direct methods using SHELXS and refined by full-matrix least-squares on F^2 using SHELXL software.[10] Non-hydrogen atoms were refined with anisotropic displacement parameters during the final cycles. Hydrogen atoms on organic molecules were placed in calculated positions with isotropic displacement parameters set to 1.2 × U_{eq} of the attached atoms. The solvent molecules are highly disordered, and attempts to locate and refine the solvent peaks were unsuccessful. For Hf–PCN-221, contributions to scattering due to these solvent molecules were removed using the SQUEEZE routine of PLATON;[11] the structure was then refined again using the data generated. Except for Zr–PCN-221 (Cu), SQUEEZE did not make the refinement results better, since there was almost no residual electron density owing to extremely weak diffractions; the structure was deposited without further treatments. The contents of the solvent region are not represented in the unit cell contents in the crystal data. Crystallographic data and structural refinements for PCN-221 are summarized in Table 1.

Table 1. Crystal Data and Structure Refinements for PCN-221

compd name	Zr–PCN-221(Cu)	Hf–PCN-221(Co)
CCDC no.	925058	925059
Formula	$C_{144}H_{72}Cu_3N_{12}O_{30}Zr_8$	$C_{144}H_{72}C_{10}Co_3Hf_8N_{12}O_{30}$
Fw	3370.52	4054.85
color	red	dark red
crystal system	cubic	cubic
space group	$Pm\bar{3}m$	$Pm\bar{3}m$
a, b, c (Å)	19.51(3)	19.152(3)
α, β, γ (deg)	90	90
V (Å^3)	7424(21)	7025(2)
Z	1	1
d_{calcd} (g/cm^3)	0.754	0.959
μ(mm^{-1})	0.515	3.151
T (K)	173(2)	110(2)
F(000)	1667	1917
reflns collected	67300	65582
independent reflns	1350	1217
obsd data [$I > 2\sigma(I)$]	728	876
data/restraints/ parameters	1350/212/59	1217/16/25
completeness (%)	99.0	98.9
GOF on F^2	1.409	1.078
$R1$, $wR2$ [$I > 2\sigma(I)$]	0.1924, 0.4359	0.1996, 0.3284
$R1$, $wR2$ (all data)	0.2450, 0.4573	0.2412, 0.3488

Activation Procedures and Gas Sorption Measurements for PCN-221. Before gas sorption experiments, as-synthesized PCN-221 (~70 mg) samples were washed with DMF three times and once with acetone and then immersed in acetone for over 12 h. Afterward, the mixture was centrifuged. After the removal of acetone by decanting, the samples were activated by drying under vacuum for 6 h and then were dried again by using the "outgas" function of the adsorption instrument for 12 h at 80 °C prior to gas adsorption/desorption measurement.

Thermal Stability Examination for PCN-221. For the thermal stability test, 5–10 mg of PCN-221 sample was heated on a TGA-50 (Shimadzu) thermogravimetric analyzer from room temperature to

dx.doi.org/10.1021/ic4018536 | Inorg. Chem. 2013, 52, 12661–12667

650 °C at a rate of 5 °C min^{-1} under N_2 flow of 50 mL min^{-1}. Both as-synthesized and activated samples for PCN-221 were measured.

Catalytic Reaction of Cyclohexane Oxidation over Zr−PCN-221(Fe). Given the presence of catalytically active porphyrinic metal centers, PCN-221 could be an ideal candidate for catalysis. Therefore, Zr−PCN-221(Fe) as a representative has been explored as a catalyst for cyclohexane oxidation. For the catalytic reaction, typically, *tert*-butyl hydroperoxide (84.7 μmol, 14 μL, 5.0−6.0 M in decane), cyclohexane (10 mL), chlorobenzene (0.1 mmol, 10 μL), and 5 mg of Zr−PCN-221(Fe) catalyst were heated at 65 °C in a 25 mL three-necked round-bottom flask. The reaction progress was monitored by taking 1−3 μL of reaction mixture for GC−FID analysis over various intervals. The reaction turnover number was calculated by dividing a summation of moles of cyclohexanol plus two times moles of cyclohexanone by moles of catalytic center (Fe).

RESULTS AND DISCUSSION

Solvothermal reactions of zirconium(IV) or hafnium(IV) chloride, M′−TCPP (M′ = Fe, Co, Cu, no metal), and benzoic acid in *N*,*N*-dimethylformamide (DMF) at 120 °C yielded cubic single crystals or polycrystalline powder of M_8O_6(M′−TCPP)$_3$ [Single crystals: M = Zr, M′ = Cu, Zr−PCN-221(Cu). Both single crystals and pure powder phase: M = Hf, M′ = Co, Hf-PCN-221(Co). Pure powder phase: M = Zr, M′ = no metal, Zr−PCN-221(no metal); M = Zr, M′ = Fe, Zr−PCN-221(Fe). PCN represents porous coordination networks]. Single-crystal and powder X-ray diffraction (XRD) studies have revealed that all PCN-221 crystallize in space group $Pm\bar{3}m$ and are isostructural. Therefore, the structure of Zr−PCN-221(Cu) will be discussed below as a representative.

The unique zirconium, in a distorted octahedral coordination environment, coordinates three oxygen atoms from three carboxylates and three μ_4-oxygen atoms (Figure 1a). Eight zirconium atoms connect six μ_4-oxygen atoms to form a Zr_8O_6 core leading to an idealized Zr_8 cube, in which the cubic vertices are occupied by zirconium atoms and the six faces are capped by six μ_4-oxygen atoms (Figure 1b). Each edge of the Zr_8 cube is bridged by a carboxylate from a TCPP ligand to give a $[Zr_8O_6(CO_2)_{12}]^{8+}$ unit with O_h symmetry. Bond-valence calculation shows that the total bond valence of a zirconium atom is +4.10, indicating the oxidation state of +4.[12] To further demonstrate the oxidation state of zirconium cations in PCN-221, X-ray photoelectron spectrum (XPS) and electron paramagnetic resonance (EPR) measurements have been conducted. As shown in Figure 2a, the positions for $3d_{3/2}$ and $3d_{5/2}$ peaks locate at 185 and 182.5 eV, respectively, which match well with those for Zr(IV) in ZrO_2.[13] In addition, EPR experiments for Zr-PCN-221(no metal) show that the signal positions are the same as those for H_2TCPP ligand (Figure 2b), revealing that the signals simply originate from the free radicals produced by the porphyrin-based ligand[14] but not zirconium cations. The weaker intensity of EPR signals in the MOF than those in the free ligand could be attributed to the lower concentrations of porphyrin center in the MOF. Both XPS and EPR results as described above confirm the assignment of the oxidation state of +4 for the zirconium, although other oxidation states are very rare.

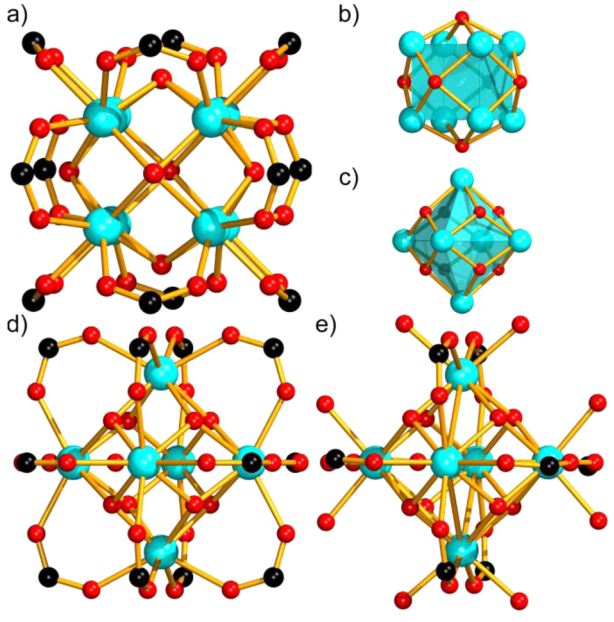

Figure 1. (a) $[Zr_8O_6(CO_2)_{12}]^{8+}$ cluster and (b) the Zr_8O_6 core in PCN-221. (c) The $Zr_6O_4(OH)_4$ core and (d) $Zr_6O_4(OH)_4(CO_2)_{12}$ building unit in PCN-56 with UiO-type structure. (e) $Zr_6(OH)_8(OH)_8(CO_2)_8$ building unit in PCN-222. The O, carboxylate O, Zr, and C atoms are shown in red, aqua, and black, respectively. The Zr_6 octahedron (b) and Zr_8 cube (c) are highlighted in aqua.

It is very interesting to compare the structures of Zr_8 and the previously reported Zr_6 clusters. As shown in Figure 1, the Zr_6 clusters have two types of coordination environments: $Zr_6O_4(OH)_4(CO_2)_{12}$[7a−f] (Figure 1d) and $Zr_6(OH)_8(OH)_8(CO_2)_8$[7g] (Figure 1e). The former has O_h symmetry and is composed of a $Zr_6O_4(OH)_4$ core coordinated by twelve carboxylate anions, while the latter has D_{4h} symmetry and is constructed with a $Zr_6(OH)_8$ core and the coordinated ligands are eight hydroxyl and eight carboxylate anions. Therefore, both Zr_6 clusters have similar cores of $Zr_6(OH)_8$ or $Zr_6O_4(OH)_4$, in which six zirconium atoms are connected by oxygen or/and hydroxyl groups to form a Zr_6 octahedron, the triangular faces of which are capped by eight μ_3-OH groups or alternatively capped by μ_3-O and μ_3-OH groups (Figure 1c). Remarkably, the zirconium and oxygen atoms exchange positions with each other in the Zr_8O_6 core in PCN-221 and the Zr_6O_8 [or $Zr_6O_4(OH)_4$] cluster core (Figure 1b,c).

The average dihedral angle between a benzene ring of a TCPP ligand and the porphyrin plane is 54.12° in previously reported Zr_6-based PCN-222.[7g] In contrast, the four peripheral benzene rings are perpendicular to the porphyrin in PCN-221, comparable to those in other reported porphyrinic MOFs.[15] Each TCPP ligand connects four Zr_8 clusters in a 4-connected mode, in which each carboxylic acid coordinates one Zr_8 cluster (Figure 3a). Similar to that of the Zr_6 cluster in UiO-type structures,[7a−f] each edge of the Zr_8 cube is bridged by one carboxylate from a TCPP ligand, so each Zr_8 cluster is 12-connected and coordinated by twelve TCPP ligands. Such connectivity leads to a three-dimensional (3D) network (Figure 3c), exhibiting a very rare (4,12)-connected **ftw** topology with point symbol of $\{4^{36}\cdot6^{30}\}\{4^4\cdot6^2\}_3$ (Figure 3b).[16] The structure features two types of polyhedral cages with pore openings of ~0.8 nm. The small cage, a slightly distorted octahedron with a cavity diameter of ~1.1 nm, comprises two Zr_8 clusters in the axial sites and four TCPP ligands in the equatorial plane (Figure 3d). The other cage, a cube with edge length of ~2.0 nm, is surrounded by eight Zr_8 clusters at the vertices and six TCPP ligands at the faces (Figure 3e). The solvent-accessible volume in PCN-221 is 70.5% calculated using the PLATON routine.[17] This provides sufficient space for solvent molecules

dx.doi.org/10.1021/ic4018536 | *Inorg. Chem.* 2013, 52, 12661−12667

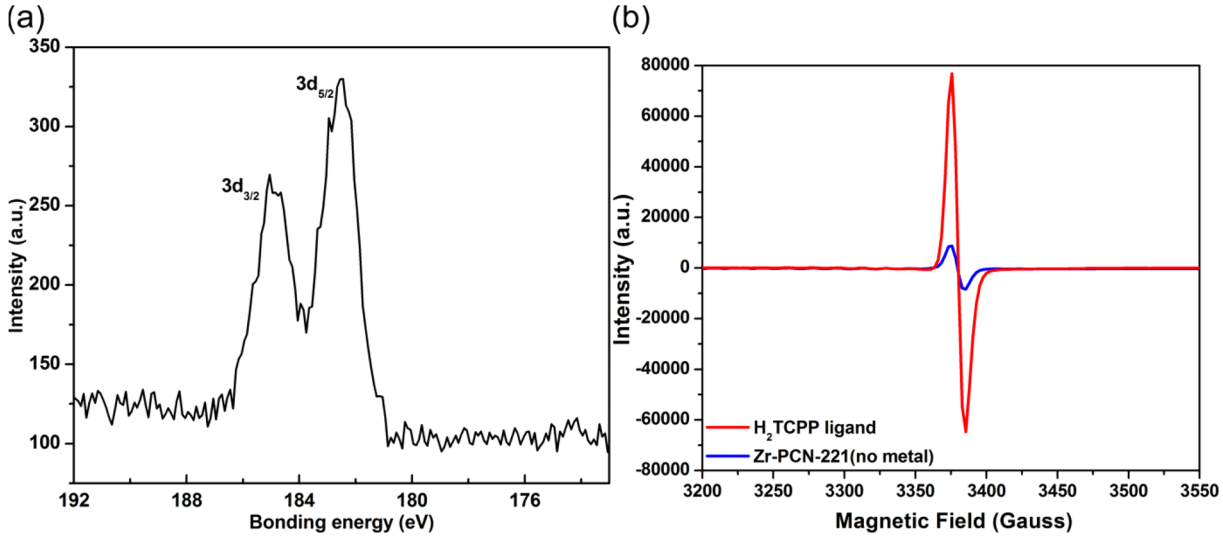

Figure 2. (a) XPS spectra for Zr−PCN-221(no metal). (b) EPR curves for H_2TCPP ligand and Zr−PCN-221(no metal).

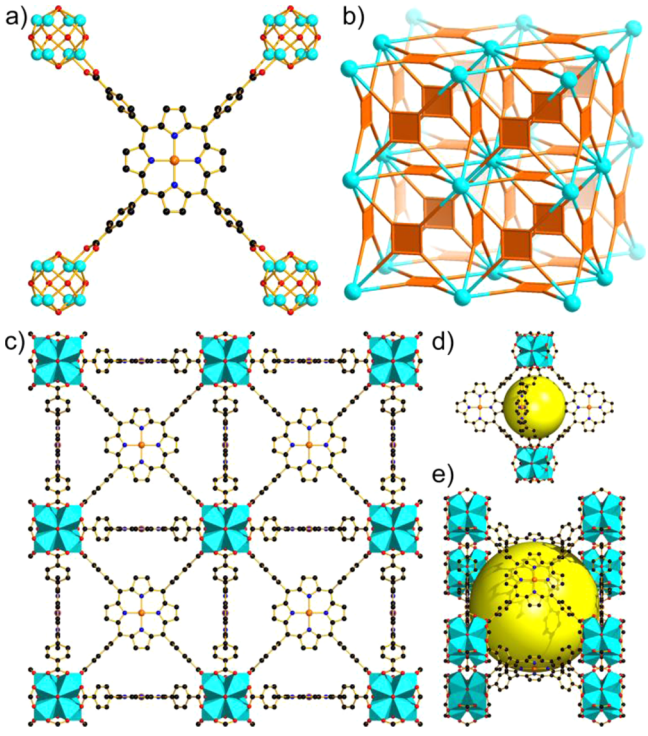

Figure 3. (a) Cu-centered TCPP ligand is 4-connected to four Zr_8 clusters. The four peripheral benzene rings are perpendicular to the porphyrinic ring in the ligand. (b) Schematic representation of the (4,12)-connected 3D network of PCN-221 with **ftw** topology, in which Zr_8 cluster and TCPP ligand are simplified as aqua dodecahedral and brown square nodes, respectively. (c) View of the 3D structure of PCN-221 along the *a*-axis. (d) Octahedral and (e) cubic cages comprised Zr_8 clusters and organic linkers in PCN-221. The space inside a cage is highlighted with a yellow sphere. The ZrO_6 polyhedra in (c−e) are shown in aqua. Color Scheme: Zr, aqua; C, dark gray; O, red; N, blue; Cu, gold. H atoms are omitted for clarity.

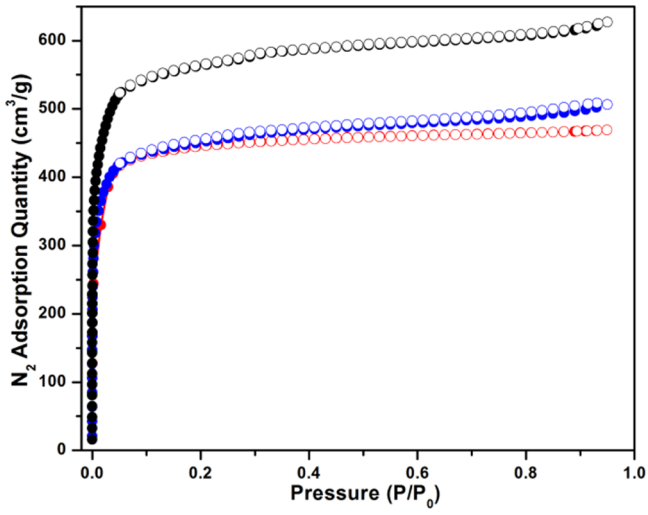

Figure 4. N_2 sorption isotherms for Zr−PCN-221(no metal) (black curves), Zr−PCN-221(Fe) (blue curves), and Hf−PCN-221(Co) (red curves).

and charge-balancing counterions for the framework, which are common in previously reported MOFs.[18]

The permanent porosity of PCN-221 has been confirmed by nitrogen adsorption experiments at 77 K (Figure 4). The typical type I isotherms suggest microporosity. The N_2 uptakes range from 450 to 650 cm^3/g (STP) and experimental pore volumes are in the range of 0.6−0.8 cm^3/g depending on what metal is coordinated by the porphyrin in PCN-221. The Brunauer−Emmett−Teller (BET) surface areas are 1936, 1549, and 1532 m^2/g for Zr−PCN-221(no metal), Zr−PCN-221(Fe), and Hf−PCN-221(Co), respectively. These values are very high for porphyrinic MOFs, as the porosity is hardly preserved upon removal of guest solvent molecules in other reported porphyrinic MOFs.[15,19] The H_2 uptakes for Zr−PCN-221(no metal), Zr−PCN-221(Fe), and Hf−PCN-221(Co) are 1.73, 1.71, and 1.62 wt % at 1 atm and 77 K, which are comparable to those of other MOFs and at the high end among those for Zr− and Hf−MOFs. The slightly lower isosteric heat of H_2 adsorption for Zr-PCN-221(no metal) than those of the other two MOFs can be attributed to the absence of exposed porphyrinic metal centers (see the Supporting Information).

The metalloporphyrin moiety within PCN-221 makes it an ideal platform for catalytic studies. Selective oxidation of cyclohexane to cyclohexanone (K) and cyclohexanol (A), key intermediates in the production of Nylon-6 and Nylon-6,6,

dx.doi.org/10.1021/ic4018536 | Inorg. Chem. 2013, 52, 12661−12667

continues to be a key and challenging process. Industrially, the process for cyclohexane oxidation was carried out at 423−433 K over cobalt-based homogeneous catalysts when air is used as oxidant, leading to about 4% conversion and 70−85% selectivity to K/A oil.[20] Achieving a high conversion while maintaining a high selectivity is very important for industrial applications.

Herein, Zr-PCN-221(Fe) was explored as a heterogeneous catalyst for cyclohexane oxidation in the presence of tert-butyl hydroperoxide (TBHP) as an oxidant at 65 °C. Based on the assumption that one mole of cyclohexanone is produced by consuming two equiv of oxidants and one mole of cyclohexanol is generated by consuming one equiv of oxidant, the reaction proceeds very quickly and completes in about 11 h, when the reaction products are obtained in almost stoichiometric amount with TBHP utilization efficiency of close to 100%. The selectivity is mainly toward cyclohexanone (86.9%) and a small amount of cyclohexanol (5.4%) is also produced, while no other oxidation products are found (Figure 5). In contrast, no

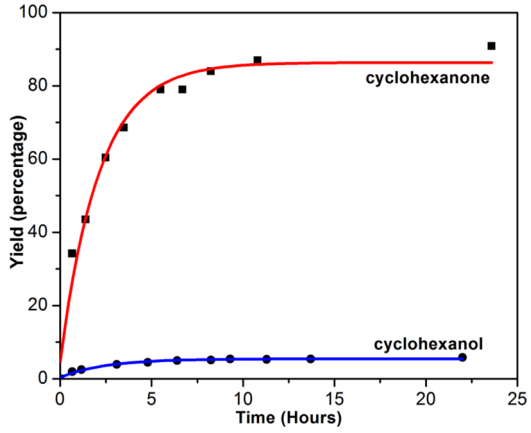

Figure 5. Catalytic oxidation of cyclohexane over Zr−PCN-221(Fe) at 65 °C. The yields are calculated on the basis of TBHP. The curves are to guide the eye and not fits to the data.

catalytic activity was observed for Zr−PCN-221(no metal). To the best of our knowledge, the total yield of K/A oil and a turnover number of 18 are comparable to or higher than those of other MOF-based or conventional molecular sieve catalysts.[21] The high reactivity and selectivity can be attributed to the high-density of accessible active porphyrinic iron(III) centers within the porous framework.

CONCLUSIONS

In summary, unprecedented Zr_8 and Hf_8 clusters have been prepared and structurally characterized for the first time in extended networks, although the molecular forms of these clusters are still unknown. Each cluster coordinates 12 TCPP ligands giving rise to highly porous 3D frameworks of PCN-221 containing two types of cavities with diameters of 1.1 and 2.0 nm. The MOFs exhibit high surface area and interesting gas sorption properties. With accessible active porphyrinic iron(III) centers, PCN-221 catalyzes the oxidation of cyclohexane with very high selectivity toward ketone and alcohol products. The discovery of Zr_8 and Hf_8 clusters not only greatly enriches cluster science, but also expands the structural diversity of Zr- and Hf-based MOFs. We believe that more and more Zr_8- and Hf_8-based MOFs with new organic linkers will be synthesized in the near future because of the unique symmetry of these clusters.

ASSOCIATED CONTENT

Supporting Information

Additional figures, table, and crystallographic data (CIF). This material is available free of charge via the Internet at http://pubs.acs.org.

AUTHOR INFORMATION

Corresponding Author

*E-mail: zhou@chem.tamu.edu.

Author Contributions

§D.F. and H.-L.J. contributed equally to this work.

Notes

The authors declare no competing financial interest.

ACKNOWLEDGMENTS

This work was supported as part of the Center for Gas Separations Relevant to Clean Energy Technologies, an Energy Frontier Research Center funded by the U.S. Department of Energy (DOE), Office of Science, Office of Basic Energy Sciences under Award Number DE-SC0001015. H.-L.J. and Z.-Y.G. was supported by U.S. Department of Energy (DE-FC36-07GO17033). D.F. and Y.P.C. was supported by the Welch Foundation (A-1725). H.-C.Z. gratefully acknowledges support from the U.S. Department of Energy (DE-AR0000073).

REFERENCES

(1) (a) Yaghi, O. M.; O'Keeffe, M.; Ockwig, N. W.; Chae, H. K.; Eddaoudi, M.; Kim, J. *Nature* **2003**, *423*, 705. (b) Férey, G.; Mellot-Draznieks, C.; Serre, C.; Millange, F.; Dutour, J.; Surblé, S.; Margiolaki, I. *Science* **2005**, *309*, 2040. (c) Horike, S.; Shimomura, S.; Kitagawa, S. *Nat. Chem.* **2009**, *1*, 695. (d) Long, J. R.; Yaghi, O. M. *Chem. Soc. Rev.* **2009**, *38*, 1213. (e) Zhou, H.-C.; Long, J. R.; Yaghi, O. M. *Chem. Rev.* **2012**, *112*, 673.

(2) (a) Ma, S.; Zhou, H.-C. *Chem. Commun.* **2010**, *46*, 44. (b) Sumida, K.; Rogow, D. L.; Mason, J. A.; McDonald, T. M.; Bloch, E. D.; Herm, Z. R.; Bae, T.-H.; Long, J. R. *Chem. Rev.* **2012**, *112*, 724. (c) Suh, M. P.; Park, H. J.; Prasad, T. K.; Lim, D.-W. *Chem. Rev.* **2012**, *112*, 782. (d) Li, J.-R.; Sculley, J.; Zhou, H.-C. *Chem. Rev.* **2012**, *112*, 869.

(3) (a) Seo, J. S.; Whang, D.; Lee, H.; Jun, S. I.; Oh, J.; Jeon, Y. J.; Kim, K. *Nature* **2000**, *404*, 982. (b) Ma, L.; Abney, C.; Lin, W. *Chem. Soc. Rev.* **2009**, *38*, 1248. (c) Farrusseng, D.; Aguado, S.; Pinel, C. *Angew. Chem., Int. Ed.* **2009**, *48*, 7502. (d) Jiang, H.-L.; Xu, Q. *Chem. Commun.* **2011**, *47*, 3351. (e) Corma, A.; García, H.; Llabrés i Xamena, F. X. *Chem. Rev.* **2010**, *110*, 4606.

(4) (a) Chen, B.; Xiang, S.; Qian, G. *Acc. Chem. Res.* **2010**, *43*, 1115. (b) Jiang, H.-L.; Tatsu, Y.; Lu, Z.-H.; Xu, Q. *J. Am. Chem. Soc.* **2010**, *132*, 5586. (c) Takashima, Y.; Martinez, V.; Furukawa, S.; Kondo, M.; Shimomura, S.; Uehara, H.; Nakahama, M.; Sugimoto, K.; Kitagawa, S. *Nat. Commun.* **2011**, *2*, 168. (d) Gu, Z.-Y.; Yang, C.-X.; Chang, N.; Yan, X.-P. *Acc. Chem. Res.* **2012**, *45*, 734−745. (e) Kreno, L. E.; Leong, K.; Farha, O. K.; Allendorf, M.; Van Duyne, R. P.; Hupp, J. T. *Chem. Rev.* **2012**, *112*, 1105.

(5) (a) An, J.; Geib, S. J.; Rosi, N. L. *J. Am. Chem. Soc.* **2009**, *131*, 8376. (b) Rocca, J. D.; Liu, D.; Lin, W. *Acc. Chem. Res.* **2011**, *44*, 957. (c) Horcajada, P.; Gref, R.; Baati, T.; Allan, P. K.; Maurin, G.; Couvreur, P.; Férey, G.; Morris, R. E.; Serre, C. *Chem. Rev.* **2012**, *112*, 1232.

(6) (a) Tranchemontagne, D. J.; Mendoza-Cortés, J. L.; O'Keeffe, M.; Yaghi, O. M. *Chem. Soc. Rev.* **2009**, *38*, 1257. (b) Perry, J. J., IV; Perman, J. A.; Zaworotko, M. J. *Chem. Soc. Rev.* **2009**, *38*, 1400.

(7) (a) Cavka, J. H.; Jakobsen, S.; Olsbye, U.; Guillou, N.; Lamberti, C.; Bordiga, S.; Lillerud, K. P. *J. Am. Chem. Soc.* **2008**, *130*, 13850. (b) Schaate, A.; Roy, P.; Godt, A.; Lippke, J.; Waltz, F.; Wiebcke, M.; Behrens, P. *Chem.—Eur. J.* **2011**, *17*, 6643. (c) Schaate, A.; Roy, P.; Preuße, T.; Lohmeier, S. J.; Godt, A.; Behrens, P. *Chem.—Eur. J.* **2011**, *17*, 9320. (d) Morris, W.; Volosskiy, B.; Demir, S.; Gándara, F.; McGrier, P. L.; Furukawa, H.; Cascio, D.; Stoddart, J. F.; Yaghi, O. M. *Inorg. Chem.* **2012**, *51*, 6443. (e) Bon, V.; Senkovskyy, V.; Senkovska, I.; Kaskel, S. *Chem. Commun.* **2012**, *48*, 8407. (f) Jiang, H.-L.; Feng, D.; Liu, T.-F.; Li, J.-R.; Zhou, H.-C. J. *J. Am. Chem. Soc.* **2012**, *134*, 14690. (g) Feng, D.; Gu, Z.-Y.; Li, J.-R.; Jiang, H.-L.; Wei, Z.; Zhou, H.-C. *Angew. Chem., Int. Ed.* **2012**, *51*, 10307. (h) Guillerm, V.; Ragon, F.; Dan-Hardi, M.; Devic, T.; Vishnuvarthan, M.; Campo, B.; Vimont, A.; Clet, G.; Yang, Q.; Maurin, G.; Férey, G.; Vittadini, A.; Gross, S.; Serre, C. *Angew. Chem., Int. Ed.* **2012**, *51*, 9267. (j) Jiang, H.-L.; Feng, D.; Wang, K.; Gu, Z.-Y.; Wei, Z.; Chen, Y.-P.; Zhou, H.-C. *J. Am. Chem. Soc.* **2013**, *135*, 13934.

(8) (a) Kickelbick, G.; Holzinger, D.; Brick, C.; Trimmel, G.; Moons, E. *Chem. Mater.* **2002**, *14*, 4382. (b) Otero, A.; Fernández-Baeza, J.; Antiñolo, A.; Tejeda, J.; Lara-Sánchez, A.; Sánchez-Barba, L.; Fernández-López, M.; López-Solera, I. *Inorg. Chem.* **2004**, *43*, 1350. (c) Baumann, S. O.; Puchberger, M.; Schubert, U. *Dalton Trans.* **2011**, *40*, 1401. (d) Gross, S. *J. Mater. Chem.* **2011**, *21*, 15853.

(9) (a) Babcock, L. M.; Day, V. W.; Klemperer, W. G. *Inorg. Chem.* **1989**, *28*, 806. (b) Dalgarno, S. J.; Atwood, J. L.; Raston, C. L. *Inorg. Chim. Acta* **2007**, *360*, 1344.

(10) APEX2 v2012.2.0 and SAINT v7.68A data collection and data processing programs, respectively. Bruker Analytical X-ray Instruments, Inc., Madison, WI; SADABS v2008/1 semi-empirical absorption and beam correction program. Sheldrick, G.M., University of Göttingen, Germany.

(11) Sheldrick, G. M. *SHELXTL*, Version 6.14, Structure Determination Software Suite, Bruker AXS, Madison, WI, 2003.

(12) (a) Brown, I. D.; Altermatt, D. *Acta Crystallogr.* **1985**, *B 41*, 244. (b) Brese, N. E.; O'Keeffe, M. *Acta Crystallogr.* **1991**, *B 47*, 192.

(13) Liao, W.; Zheng, T.; Wang, P.; Tu, S.; Pan, W. *J. Environ. Sci.* **2010**, *22*, 1800.

(14) Lan, M.; Zhao, H.; Yuan, H.; Jiang, C.; Zuo, S.; Jiang, Y. *Dyes Pigments* **2007**, *74*, 357.

(15) (a) Farha, O. K.; Shultz, A. M.; Sarjeant, A. A.; Nguyen, S. T.; Hupp, J. T. *J. Am. Chem. Soc.* **2011**, *133*, 5652. (b) Lee, C. Y.; Farha, O. K.; Hong, B. J.; Sarjeant, A. A.; Nguyen, S. T.; Hupp, J. T. *J. Am. Chem. Soc.* **2011**, *133*, 15858. (c) Burnett, B. J.; Barron, P. M.; Hu, C.; Choe, W. *J. Am. Chem. Soc.* **2011**, *133*, 9984. (d) Yang, X.-L.; Xie, M.-H.; Zou, C.; He, Y.; Chen, B.; O'Keeffe, M.; Wu, C.-D. *J. Am. Chem. Soc.* **2012**, *134*, 10638.

(16) (a) O'Keeffe, M.; Delgado-Friedrichs, O.; Yaghi, O. M. *Acta Crystallogr.* **2006**, *A 62*, 350. (b) Chang, Z.; Zhang, D.-S.; Hu, T.-L.; Bu, X.-H. *Cryst. Growth Des.* **2011**, *11*, 2050. (c) Zhao, X.; Wang, X.; Wang, S.; Dou, J.; Cui, P.; Chen, Z.; Sun, D.; Wang, X.; Sun, D. *Cryst. Growth Des.* **2012**, *12*, 2736.

(17) Spek, A. L. *J. Appl. Crystallogr.* **2003**, *36*, 7.

(18) (a) Fei, H.; Rogow, D. L.; Oliver, S. R. J. *J. Am. Chem. Soc.* **2010**, *132*, 7202. (b) Zheng, S.-T.; Bu, J. J.; Wu, T.; Chou, C.; Feng, P.; Bu, X. *Angew. Chem., Int. Ed.* **2011**, *50*, 8858. (c) Zheng, S.-T.; Wu, T.; Zuo, F.; Chou, C.; Feng, P.; Bu, X. *J. Am. Chem. Soc.* **2012**, *134*, 1934.

(19) (a) Fateeva, A.; Devautour-Vinot, S.; Heymans, N.; Devic, T.; Grenèche, J.-M.; Wuttke, S.; Miller, S.; Lago, A.; Serre, C.; Weireld, G. D.; Maurin, G.; Vimont, A.; Férey, G. *Chem. Mater.* **2011**, *23*, 4641. (b) Wang, X.-S.; Chrzanowski, M.; Gao, W.-Y.; Wojtas, L.; Chen, Y.-S.; Zaworotko, M. J.; Ma, S. *Chem. Sci.* **2012**, *3*, 2823.

(20) (a) Weissermel, K.; Arpe, H.-J. *Industrial Organic Chemistry*, 2nd ed.; VCH Press: Weinheim, 1993. (b) Herejgers, B. P. C.; Weckhuysen, B. M. *J. Catal.* **2010**, *270*, 16.

(21) (a) Grootboom, N.; Nyokong, T. *J. Mol. Catal. A: Chem.* **2002**, *179*, 113. (b) Alkordi, M. H.; Liu, Y.; Larsen, R. W.; Eubank, J. F.; Eddaoudi, M. *J. Am. Chem. Soc.* **2008**, *130*, 12639. (c) Maksimchuk, N. V.; Kovalenko, K. A.; Fedin, V. P.; Kholdeeva, O. A. *Chem. Commun.* **2012**, *48*, 6812.